

How Shall We Go to Mars? A Review of Mission Scenarios

Gerald Walberg*

North Carolina State University, Raleigh, North Carolina 27695

Various scenarios for manned Mars missions are reviewed, and four mission classes—opposition, conjunction, fast-transfer conjunction, and split sprint—are identified as contenders for the initial missions. These four mission classes are then compared with regard to three factors: 1) reduced gravity effects, 2) exposure to space radiation, and 3) initial mass in Earth orbit. It is concluded that the choice of mission scenario depends to a large extent on the amount of physical deconditioning caused by long-term exposure to the 3/8 Earth gravity environment of the Martian surface. Although important, exposure to space radiation is not a clear discriminator because the various scenarios yield roughly comparable radiation doses and even with conservative assumptions, none of them, significantly exceed the National Council on Radiation Protection and Measurement limits. If it is assumed that 3/8 Earth gravity is as harmful as zero gravity, the only acceptable mission scenario is the split sprint, which is truly attractive only when a high specific impulse propulsion system, such as nuclear thermal propulsion, is used. If, on the other hand, it is assumed that during their stay on the Martian surface the astronauts experience no further deconditioning, the mission scenario of choice is the fast-transfer conjunction class because of its low radiation doses, short exposure to zero gravity, and low Earth departure masses for either chemical propulsion with aerobraking or nuclear thermal propulsion.

Nomenclature

| | |
|----------------------|---|
| a, b | =factors determined from regression of historical cost data, used in TRANSCOST |
| D | =blood-forming organ radiation dose, rem |
| F_S, F_E | =fabrication cost-estimating relationships for stages and propulsion systems, respectively, used in TRANSCOST |
| f_1, f_2, f_3, f_4 | =corrective factors used in TRANSCOST cost-estimating relationships to account for technology status, etc. |
| g | =acceleration due to gravity at Earth's surface, 9.807 m/s ² |
| H_S, H_E | =development cost-estimating relationships for stages and propulsion systems, respectively, used in TRANSCOST |
| I_{sp} | =specific impulse, s |
| M | =vehicle stage or propulsion system dry mass, used in TRANSCOST, kg |
| m | =vehicle or payload mass, see Eqs. (1–8), kg |
| N | =number of vehicle stages, used in TRANSCOST |
| n | =number of identical units (e.g., engines) per stage, used in TRANSCOST |
| V_M, V_E | =entry velocities at Mars and Earth, respectively, km/s |
| x, y | =factors determined from regression of historical cost data, used in TRANSCOST |
| β | = $e^{1.05 DV/gI_{sp}}$, see Eq. (5) |

| | |
|------------|--|
| ΔV | =velocity increment, km/s |
| γ | =aerobrake mass factor, $(m_{AB} + m_{p/L})/m_{p/L}$ |
| λ | =structural mass factor, $(m_s + m_p)/m_p$ |
| ψ | =overall mass factor for a propulsive stage, $m/m_{p/L}$, see Eq. (6) |

Subscripts

| | |
|-------|--------------------------------|
| AB | =aerobrake |
| E | =Earth return |
| ERM | =Earth return module |
| HAB | =habitation module |
| M | =Mars arrival |
| MEM | =Mars excursion module |
| MID | =midcourse burn |
| p/L | =payload |
| p | =propellant |
| s | =structure |
| TMI | =trans-Mars injection |
| 1 | =Earth departure |
| 2 | =outbound midcourse ΔV |
| 3 | =Mars arrival |
| 4 | =Mars departure |
| 5 | =Earth return |

Introduction

MANNED missions to Mars have been dreamed of since the turn of the century and have been studied seriously since the early 1960s when NASA proposed such a mission as the next



Gerald D. Walberg, Professor of Mechanical and Aerospace Engineering at North Carolina State University, received his B.S. and M.S. degrees from Virginia Polytechnic Institute and State University and Ph.D. from North Carolina State University. Dr. Walberg is Deputy Director of the Mars Mission Research Center and Director of the North Carolina Space Grant Consortium. He teaches and carries out research in the areas of hypersonic gas-dynamics, planetary mission analysis, and spacecraft design. Prior to assuming his present position, he worked for 32 years at the NASA Langley Research Center where he carried out individual research and held numerous management positions including Head of the Aerothermodynamics Branch, Chief of the Space Systems Division and Deputy Director for Space. Following retirement from NASA, and prior to joining the faculty at North Carolina State University, he taught at the George Washington University/NASA Joint Institute for Advancement of Flight Sciences. He is a fellow of the AIAA and has served as Associate Editor of the Journals of Spacecraft and Rockets and Thermophysics and Heat Transfer and as a member of the AIAA Technical Committees on Space Systems and Space Transportation.

Presented as Paper 92-0841 at the AIAA 30th Aerospace Sciences Meeting, Reno, NV, Jan. 6–9, 1992; received March 6, 1992; revision received Dec. 19, 1992; accepted for publication Dec. 19, 1992. Copyright © 1992 by North Carolina State University. Published by the American Institute of Aeronautics and Astronautics, Inc., with permission.

*Professor, Department of Mechanical and Aerospace Engineering, and Deputy Director, Mars Mission Research Center. Fellow AIAA.

| Mission Times (days) | | ΔV 's (km/s) | |
|----------------------|-----------|----------------------|-------------|
| Outbound | 172 - 334 | TMI | 3.72 - 4.89 |
| Stopover | 60 | M | 1.78 - 3.93 |
| Inbound | 250 - 375 | TEI | 1.24 - 3.30 |
| Total | 531-714 | E | 3.77 - 5.20 |

| Entry Velocities (km/s) | |
|-------------------------|---------------|
| M | 6.42 - 8.58 |
| E | 11.39 - 12.80 |

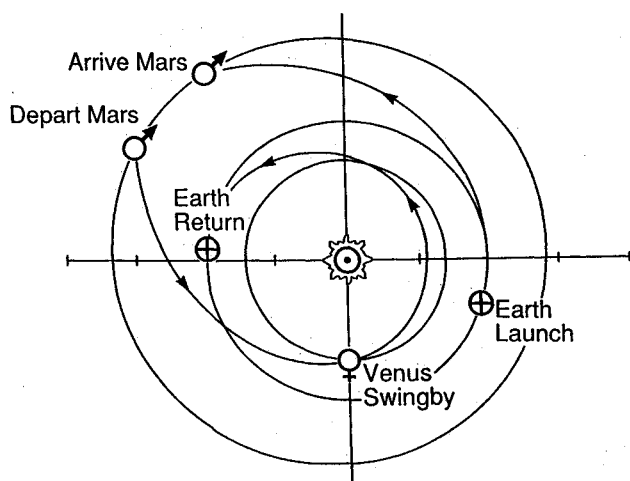


Fig. 1 Opposition-class missions with Venus swingbys: 2002–15.

| Mission Times (days) | | ΔV 's (km/s) | |
|----------------------|------------|----------------------|-------------|
| Outbound | 202 - 402 | TMI | 3.50 - 3.85 |
| Stopover | 286 - 551 | M | 0.80 - 2.59 |
| Inbound | 191 - 335 | TEI | 0.73 - 1.44 |
| Total | 935 - 1025 | E | 3.52 - 4.49 |

| Entry Velocities (km/s) | |
|-------------------------|---------------|
| M | 5.44 - 7.23 |
| E | 11.13 - 12.10 |

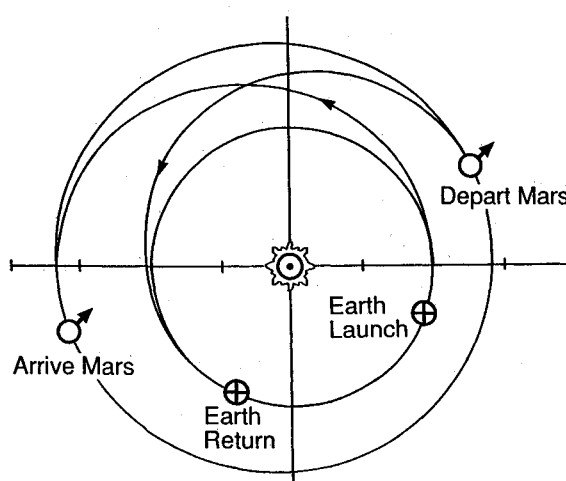


Fig. 2 Conjunction-class missions: 2003–18.

major space initiative following the Apollo program. More recently, interest in a manned mission to Mars was rekindled by a series of studies and planning activities aimed at charting the nation's future directions in space. This activity culminated in the proposal by President Bush of the Space Exploration Initiative, which would return us to the moon and then send us onward to Mars.

Over the past 30 years, many different Mars mission scenarios have been put forward. A wide variety of trajectory, propulsion, and spacecraft design options have been proposed, ranging from chemically powered/aerobraking or nuclear-powered fast-transfer missions with durations of 1.0–1.5 yr to low-thrust electrically powered or solar sail missions with trip times around 3 yr to missions featuring cycler spacecraft with lengthy Mars stay times and total durations of 5–6 yr. Each of these approaches has distinct advantages and some drawbacks. The current paper reviews the various mission scenarios with special emphasis on the early missions to Mars and on three factors that may be decisive in determining the ultimate choice of mission scenario: 1) reduced gravity effects, 2) exposure to space radiation and 3) initial mass in Earth orbit.

Mission Scenarios

The number of ways in which a manned mission to Mars can be carried out is apparently limited only by human imagination, and the details of the various scenarios that have been proposed cannot begin to be covered in a single brief presentation. However, most of the major themes and variations can be grouped into the following broad categories: 1) high-thrust opposition-class missions, 2) high-thrust conjunction-class missions, 3) split missions, 4) low thrust missions, 5) missions using extraterrestrial propellants, and 6) cycling spacecraft.

Each of these mission categories will now be described briefly and discussed. These mission categories are essentially those used by Niehoff¹ and Hoffman et al.,² and the reader is referred to these references for more complete discussions. The typical mission characteristics were taken from Refs. 2 and 3 and are presented in Tables 1–4. Figures 1–8 are also patterned after figures presented originally in Refs. 2 and 3. The velocity increments ΔV presented

in Tables 1–4 are computed under the assumption of a 500-km circular Earth orbit and a 1-sol Mars parking orbit.

High-Thrust Opposition-Class Missions

Figure 1 and Table 1 illustrate the opposition-class missions. To reduce mission duration to the range of 1.5–2.0 yr, a fast transfer is flown on either the outbound or inbound leg, usually taking advantage of a Venus swingby opportunity to reduce ΔV requirements and entry velocities. Such missions typically have stay times at Mars of 30–60 days. In Ref. 4, Braun et al. showed that in the 2010–25 time frame, relatively low energy mission opportunities occur approximately every two years with relatively low entry velocities at both Mars (≤ 8.6 km/s) and Earth (≤ 12.5 km/s). Hence, such missions are good candidates for aerobraking, especially at Mars. The characteristics of a complete cycle of opposition-class missions spanning the 2002–15 time frame are presented in Table 1 and summarized in Fig. 1. Note that during the fast-transfer mission leg the spacecraft flies inside the orbits of both Earth and Venus and hence comes relatively close (0.6–0.7 AU) to the sun. Should a solar flare occur during this time, the crew would have to be protected from an increased radiation dose.

High-Thrust Conjunction-Class Missions

The conjunction-class missions illustrated in Table 2 and Fig. 2 are the least energetic of the Mars mission scenarios. Actually, the transfer times to and from Mars are only slightly longer than those of the opposition-class missions. The long overall mission durations result from the long mandatory Mars stay times that are required by Mars-Earth phasing.

A recent study³ has shown that the transit times for conjunction-class missions may be reduced by up to 100 days for a very modest (~5%) increase in departure ΔV . These missions are often called fast-transfer conjunction-class missions. The characteristics of a cycle of fast-transfer conjunction-class missions, based on data from Ref. 3, are presented in Table 3. Conjunction-class missions lie entirely outside the Earth's orbit and hence require less protection from solar flares. Were it not for subjecting the crew to an extended exposure to reduced gravity on the Martian surface, the conjunction-class mission would be the clear choice for early missions to Mars.

Table 1 Opposition-class missions

| Earth-departure date | ΔV_{TMI}^a , km/s | Outbound flight time, days | ΔV_{MID}^a , km/s | ΔV_M^b , km/s | Mars stay time, days | ΔV_{TEI}^b , km/s | ΔV_{MID}^a , km/s | Return flight time, days | ΔV_E^a , km/s | Total mission time, days |
|----------------------|---------------------------|----------------------------|---------------------------|-----------------------|----------------------|---------------------------|---------------------------|--------------------------|-----------------------|--------------------------|
| Aug. 7, 2002 | 3.713 | 307.90 | VS ^c | 3.930 | 60 | 2.019 | 0.0 | 257.90 | 5.196 | 625.8 |
| June 5, 2004 | 4.098 | 334.20 | VS | 3.278 | 60 | 1.415 | 0.0 | 266.10 | 2.774 | 660.3 |
| Aug. 29, 2007 | 4.744 | 172.10 | 0.0 | 3.930 | 60 | 3.067 | VS | 329.80 | 4.093 | 561.9 |
| Feb. 7, 2008 | 4.345 | 278.80 | VS + 0.61 | 3.388 | 60 | 1.956 | VS | 374.70 | 4.056 | 713.5 |
| Nov. 25, 2010 | 4.357 | 287.80 | VS | 3.930 | 60 | 1.242 | 0.0 | 361.40 | 5.196 | 709.2 |
| Nov. 20, 2013 | 3.766 | 256.30 | 0.0 | 1.777 | 60 | 3.145 | VS | 310.80 | 4.087 | 627.1 |
| Nov. 23, 2015 | 4.893 | 220.60 | 0.0 | 3.930 | 60 | 3.296 | VS | 249.90 | 5.196 | 530.5 |

^a500-km circular Earth orbit. ^b1-sol Mars orbit. ^cVS=Venus swingby.

Table 2 Conjunction-class missions

| Earth-departure date | ΔV_{TMI}^a , km/s | Outbound flight time, days | ΔV_{MID}^a , km/s | ΔV_M^b , km/s | Mars stay time, days | ΔV_{TEI}^b , km/s | Return flight time, days | ΔV_{MID}^a , km/s | ΔV_E^a , km/s | Total mission time, days |
|----------------------|---------------------------|----------------------------|---------------------------|-----------------------|----------------------|---------------------------|--------------------------|---------------------------|-----------------------|--------------------------|
| June 7, 2003 | 3.554 | 201.70 | 0.0 | 0.908 | 550.70 | 1.444 | 192.30 | 0.0 | 3.770 | 994.70 |
| Sept. 1, 2005 | 3.848 | 401.90 | 0.0 | 1.339 | 285.60 | 1.161 | 283.10 | 0.0 | 3.549 | 970.60 |
| Sept. 22, 2007 | 3.729 | 368.50 | 0.0 | 0.964 | 307.60 | 0.956 | 296.90 | 0.0 | 3.519 | 973.00 |
| Oct. 14, 2009 | 3.620 | 327.50 | 0.0 | 0.797 | 539.80 | 0.859 | 332.50 | 0.0 | 3.712 | 999.80 |
| Nov. 8, 2011 | 3.561 | 297.60 | 0.0 | 0.930 | 391.80 | 0.768 | 335.30 | 0.0 | 4.232 | 1024.70 |
| Jan. 1, 2014 | 3.553 | 328.80 | 0.0 | 1.936 | 382.70 | 0.734 | 300.20 | 0.0 | 4.488 | 1011.70 |
| March 21, 2016 | 3.518 | 305.30 | 0.0 | 2.588 | 417.70 | 0.796 | 212.40 | 0.0 | 3.616 | 935.40 |
| May 17, 2018 | 3.506 | 235.10 | 0.0 | 1.198 | 515.40 | 1.266 | 191.20 | 0.0 | 3.648 | 941.70 |

^a500-km circular earth orbit. ^b1-sol Mars orbit.

Table 3 Fast-transfer conjunction-class missions

| Earth-departure date | ΔV_{TMI}^a , km/s | Outbound flight time, days | ΔV_{MID}^a , km/s | ΔV_M^b , km/s | Mars stay time, days | ΔV_{TEI}^b , km/s | Return flight time, days | ΔV_{MID}^a , km/s | ΔV_E^a , km/s | Total mission time, days |
|-----------------------------|---------------------------|----------------------------|---------------------------|-----------------------|----------------------|---------------------------|--------------------------|---------------------------|-----------------------|--------------------------|
| June 5 ^c , 2018 | 4.287 | 100 | 0.0 | 3.878 | 666 | 2.175 | 120 | 0.0 | 5.145 | 886 |
| July 5 ^c , 2020 | 4.217 | 139 | 0.0 | 3.050 | 630 | 2.180 | 150 | 0.0 | 5.484 | 919 |
| Sept. 6 ^c , 2022 | 4.051 | 181 | 0.0 | 2.131 | 540 | 1.684 | 190 | 0.0 | 5.233 | 911 |
| Oct. 12 ^c , 2024 | 4.025 | 194 | 0.0 | 2.654 | 515 | 1.352 | 210 | 0.0 | 5.329 | 919 |
| Nov. 24, 2011 | 3.836 | 190 | 0.0 | 3.696 | 512 | 0.986 | 220 | 0.0 | 5.241 | 922 |
| Jan. 1, 2014 | 3.672 | 181 | 0.0 | 3.816 | 555 | 1.069 | 180 | 0.0 | 5.417 | 916 |
| March 3, 2016 | 3.687 | 150 | 0.0 | 3.822 | 635 | 1.699 | 120 | 0.0 | 5.482 | 905 |

^a500-km circular earth orbit. ^b1-sol Mars orbit. ^cSimilar missions assumed at 15-yr intervals.

Table 4 Split-sprint missions

| Earth-departure date | ΔV_{TMI}^a , km/s | Outbound flight time, days | ΔV_{MID}^a , km/s | ΔV_M^b , km/s | Mars stay time, days | ΔV_{TEI}^b , km/s | Return flight time, days | ΔV_{MID}^a , km/s | ΔV_E^a , km/s | Total mission time, days |
|-------------------------------|---------------------------|----------------------------|---------------------------|-----------------------|----------------------|---------------------------|--------------------------|---------------------------|-----------------------|--------------------------|
| June 7, 2003 (C) ^d | | | | | | | | | | |
| Oct 9, 2004 (M) | 4.013 | 264.6 | 2.31 | 3.930 | 30 | 1.991 | 145.4 | 0.0 | 4.257 | 440 |
| Sept. 1, 2005 (C) | | | | | | | | | | |
| Dec. 11, 2006 (M) | 4.938 | 238.1 | 2.38 | 3.930 | 30 | 2.188 | 171.9 | 0.0 | 4.257 | 440 |
| Sept. 22, 2007 (C) | | | | | | | | | | |
| Jan. 28, 2009 (M) | 5.073 | 246.1 | VS+1.66 | 3.930 | 30 | 3.710 | 163.9 | 0.0 | 4.257 | 440 |
| Oct. 14, 2009 (C) | | | | | | | | | | |
| March 12, 2011(M) | 6.037 | 253.2 | 3.31 | 3.930 | 30 | 4.211 | 156.8 | 0.0 | 4.256 | 440 |
| Nov. 8, 2011 (C) | | | | | | | | | | |
| March 30, 2013 (M) | 5.571 | 268.0 | 3.47 | 3.930 | 30 | 3.501 | 162.0 | 0.0 | 4.256 | 935.40 |
| Jan. 1, 2014 (C) | | | | | | | | | | |
| April 20, 2015 (M) | 5.056 | 287.9 | 3.40 | 3.928 | 30 | 2.256 | 152.1 | 0.0 | 4.232 | 935.40 |
| March 21, 2016 (C) | | | | | | | | | | |
| Aug. 29, 2001 (M) | 4.199 | 274.2 | VS ^c | 3.930 | 30 | 2.275 | 135.8 | 0.0 | 3.706 | 941.70 |

^a500-km circular earth orbit. ^b1-sol Mars orbit. ^cVS=Venus swingby. ^d(C)=Cargo mission—see Table 2 for characteristics.
^e(M)=Manned mission. ^fSimilar missions assumed at 15 year intervals.

| Mission Times (days) | | ΔV 's (km/s) | |
|----------------------|-----------|----------------------|-------------|
| Outbound | 238 - 287 | TMI | 4.01 - 6.04 |
| Stopover | 30 | Midcourse | VSB - 3.47 |
| Inbound | 145 - 172 | M | 3.93 |
| Total | 440 - 470 | TEI | 1.99 - 4.21 |
| | | E | 3.71 - 4.26 |

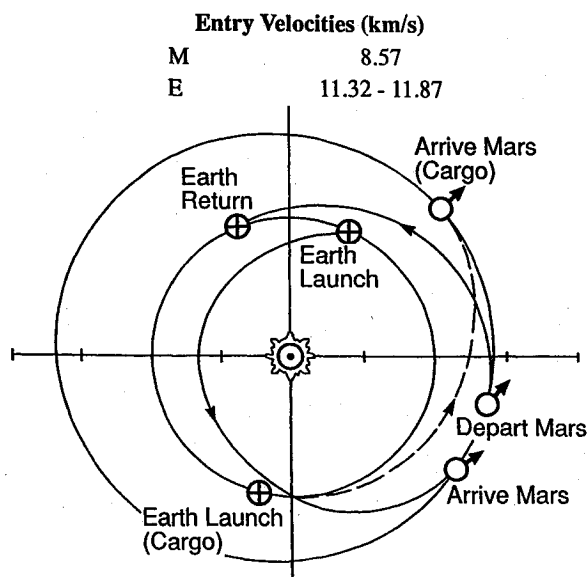


Fig. 3 Split sprint missions: 2002-15.

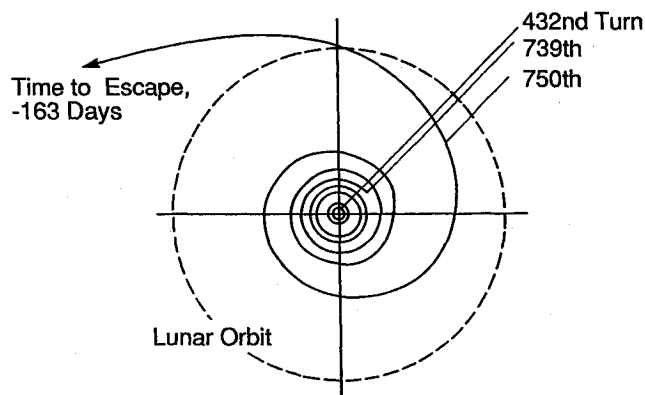
Split Missions

The basic idea of the split mission scenario is to transport most of the payload to Mars (including the return propellant) on an unmanned cargo vehicle flying an efficient conjunction-class transfer and to transport the crew on a high-energy, fast-transfer, opposition-class (sprint) trajectory launched after the cargo vehicle is safely in Mars orbit. In this way, the duration of the manned mission can be shortened to 1.0-1.5 yr without unduly increasing the mass that must be initially placed in Earth orbit. Figure 3 and Table 4 illustrate the split sprint mission scenario. Each sprint mission in Table 3 is paired with a preceding conjunction-class mission from Table 2. The duration of the manned mission is reduced, which is desirable because it reduces the overall exposure to reduced gravity to time periods comparable to the Soviet MIR missions (1 yr). The manned transfer legs have all of the advantages and disadvantages of highly energetic opposition-class missions.

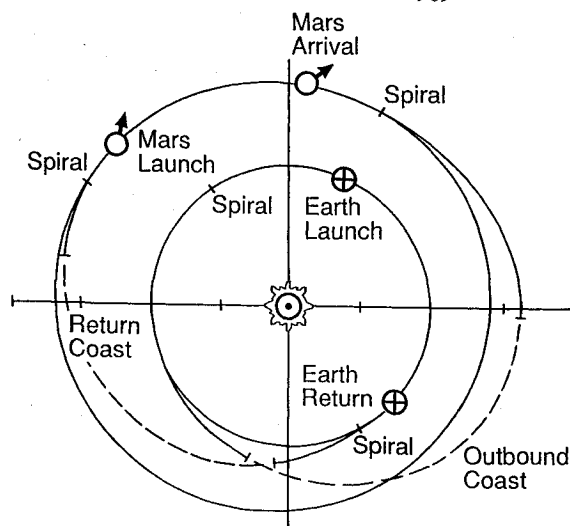
Low-Thrust Missions

In the missions discussed up to this point, the ΔV increments are achieved by short-duration burns of high-thrust rockets. Hence they can be modeled as impulsive velocity additions, greatly simplifying the trajectory analysis. On the other hand, low-thrust systems such as solar electric or nuclear electric thrusters or solar sails achieve their ΔV increments during long duration spirals about the departure and arrival planets as well as low-level thrusting during portions of the interplanetary transfer. Figures 4a and 4b illustrate low-thrust mission scenarios. Figure 4a, which is based on data from Ref. 5, illustrates a typical Earth-escape spiral. Note that the vehicle spends a large amount of time in the Earth's radiation belts. Hence, for a manned mission the crew would not be on board initially. Instead, using an Earth-launched shuttle craft, the crew would rendezvous with the low-thrust vehicle after it emerged from the radiation belts. For the example shown in Fig. 4a, this would be after the low-thrust vehicle had been spiraling for about 100 days. Figure 4b illustrates a typical low-thrust mission scenario. In this case (which is taken from Ref. 1), the thrust level is somewhat higher than that depicted in Fig. 4a. Hence, the Earth-escape spiral lasts 52 days in Fig. 4b as opposed to 163 days in Fig. 4a. Note that after Earth escape, in Fig. 4b, the vehicle continues to thrust and is eventually placed in a relatively high energy transfer

to Mars. Accordingly, an extended retrothrusting period is required on Mars approach. Using such an approach results in a mission duration that is shorter than that typical of a conjunction-class mission and provides Mars stay times that are intermediate to those for opposition- and conjunction-class missions, i.e., 100-200 days. The great virtue of the low-thrust systems is their high specific impulse (thousands of seconds) that greatly reduces the amount of fuel that must be placed in low-Earth orbit. Low-thrust vehicles are obviously well suited to cargo missions (assuming the cargo is not adversely affected by passage through the radiation belts). Hence, an attractive type of split mission is one in which the cargo vehicle uses low thrust propulsion and the manned vehicle uses high-thrust chemical or nuclear propulsion and flies an opposition-class trajectory. The mission scenarios presented in Figs. 4a and 4b are representative of conjunction-class missions with near-term electric propulsion systems that, although not flight demonstrated, have reached a high level of maturity in ground tests. It should be pointed out that foreseeable advances in electric propulsion can result in dramatic reductions in trip times. In Ref. 6, it is shown that a nuclear electric system, consisting of a "growth" SP-100 reactor with potassium Rankine power conversion (modified to have a shortened full power life of 2 yr) and argon ion thrusters

Fig. 4a Low-thrust Earth escape.^{1,5}

| Mission Times (days) | |
|----------------------|-----|
| Earth Spiral | 52 |
| Outbound | 510 |
| Mars Spiral | 39 |
| Stopover | 100 |
| Mars Spiral | 23 |
| Inbound | 229 |
| Earth Spiral | 16 |
| Total | 969 |

Fig. 4b Typical low-thrust mission.¹

employed in a split sprint mission scenario, is capable of piloted trip times on the order of 500 days.

Missions Using Extraterrestrial Propellants

One of the primary challenges of the opposition- and conjunction-class missions is that they require transporting large amounts of propellant through the Earth's deep gravity well to the low-Earth staging orbit. To avoid this, numerous studies have considered using propellants produced on the moon, on Mars, or on the Martian satellite Phobos. To use these extraterrestrial propellants effectively, staging points other than the conventional Earth and Mars parking orbits are often used. For instance, scenarios involving the use of lunar oxygen often use one of the Earth-moon libration points. An example of this is illustrated in Fig. 5. In this case a chemically propelled Mars mission vehicle, the crew, and the necessary hydrogen fuel are transported from Earth to the L1 libration point. The liquid oxygen, on the other hand, is produced from lunar regolith and transported to L1. Once the Mars vehicle is loaded with oxidizer, a small burn places the vehicle in an L1-Earth transfer trajectory. At perigee, a second burn injects the vehicle into its trans-Mars trajectory. Since the energy required to transport the massive liquid oxygen from the moon to L1 is much less than that required to transport the same amount of oxygen from the Earth's surface to low-Earth orbit (LEO), the overall energy requirements for staging a Mars mission in this way are significantly reduced. Of course, such an approach requires the establishment of an extensive infrastructure, including the lunar production and launch facilities and the L1 staging base. Hence, such a scenario is a candidate for far term missions rather than the initial visits to Mars.

Since oxygen and hydrogen may be extractable from the regolith of Mars and Phobos, and CO_2 is available in the Martian atmosphere, there are multiple possibilities for producing return-trip propellants at Mars or Phobos. An interesting possibility, illustrated in Fig. 6, is to use Phobos itself as a Mars staging base. Rather than the spacecraft being placed into a parking orbit about

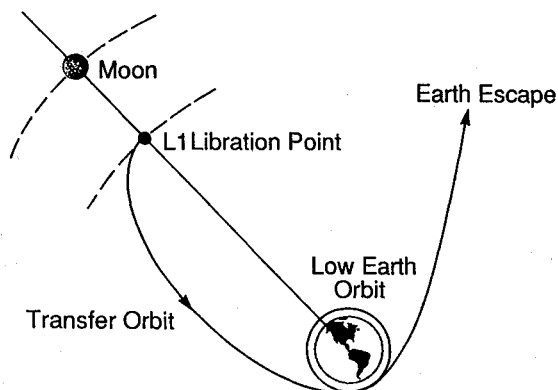


Fig. 5 Staging from L1 libration point.

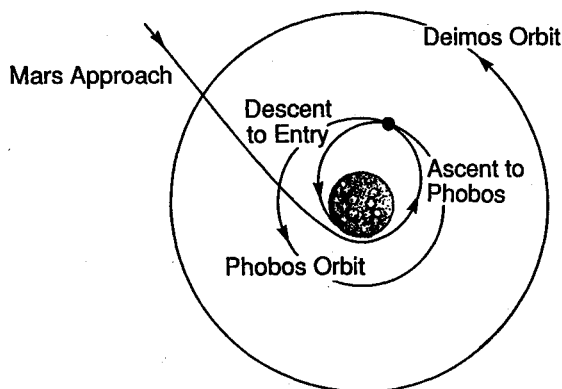


Fig. 6 Mars staging from Phobos.

| Mission Times (days) | | ΔV 's (km/s) | |
|----------------------|-------------|----------------------|-------------|
| Outbound | 221 - 1101 | TMI | 3.94 - 4.04 |
| Stopover | 1331 - 1352 | M | 1.50 - 1.69 |
| Inbound | 197 - 1193 | TEI | 1.50 - 1.69 |
| Total | 1849 - 2545 | E | 3.94 - 4.04 |

Entry Velocities (km/s)

| | |
|---|---------------|
| M | 6.14 - 6.33 |
| E | 11.56 - 11.65 |

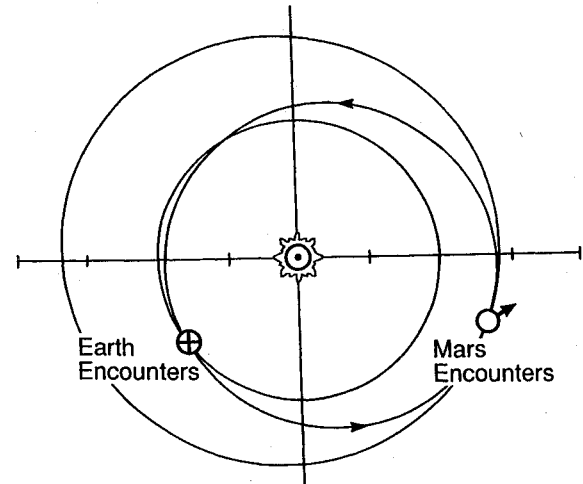


Fig. 7 Visit 1 trajectory—one cycling spacecraft: 2001–16.

| Mission Times (days) | | ΔV 's (km/s) | |
|----------------------|-------------|----------------------|-------------|
| Outbound | 148 - 169 | TMI | 4.47 - 4.72 |
| Stopover | ~ 730 | M | 3.11 - 8.06 |
| Inbound | 146 - 170 | TEI | 3.55 - 7.92 |
| Round Trip | 1020 - 1069 | E | 4.43 - 4.72 |

Entry Velocities (km/s)

| | |
|---|---------------|
| M | 7.75 - 12.70 |
| E | 12.04 - 12.33 |

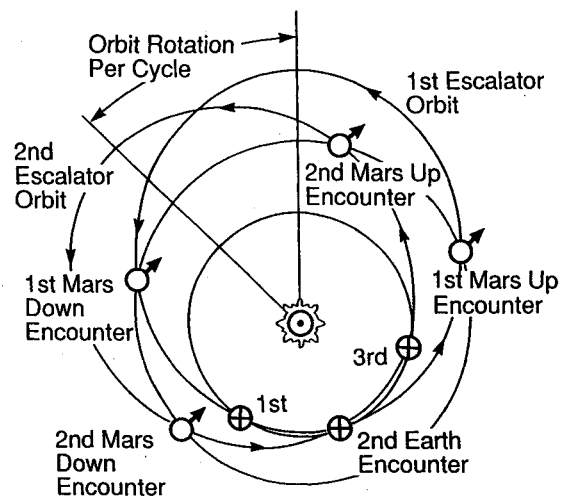


Fig. 8 Up-escalator, down-escalator scenario—two cycling spacecraft: 2001–16.

Mars, it actually makes a rendezvous with Phobos. Propellant manufactured on Phobos is then used to fuel the Earth return spacecraft. From Phobos, the crew could descend to the surface of Mars or they could send automated rovers remotely controlled from Phobos to explore the Martian surface.

Finally, the so-called Mars direct scenario warrants mention. In this scenario proposed by Zubrin and Baker,⁷ hydrogen carried to Mars aboard an unmanned precursor spacecraft is reacted with CO₂ from the Martian atmosphere to produce CH₄ and H₂O. The H₂O is then electrolyzed to produce oxygen. Additional oxygen is produced by direct dissociation of Martian atmospheric CO₂. All of this is powered by a 10-kW nuclear reactor and produces sufficient methane/oxygen propellants to fuel a small Earth-return vehicle. The hydrogen, nuclear reactor, fuel-processing plant, and Earth-return vehicle are all transported to Mars by a single shuttle-derived heavy lift vehicle launched directly from the Earth's surface. Once successful production of the Earth-return propellant is verified, two more vehicles are launched directly from Earth. One of these transports the crew, a habitation module, provisions for 3 yr, and an oxygen-methane powered surface rover to Mars. The second contains a backup fuel production plant and Earth-return vehicle identical to that already in place on Mars. By using Mars-produced Earth-return propellants, the initial mass of the trans-Mars vehicle is reduced to the point that direct launch from the Earth's surface rather than assembly in Earth orbit is feasible.

Cycling Spacecraft

In conventional mission scenarios, large amounts of energy are expended in accelerating and decelerating the massive habitation module required for a manned mission. The basic concept of cycling spacecraft derives from the thought that the large interplanetary spacecraft could be placed in a stable orbit that would regularly encounter the Earth and Mars. Then transport to and from the surfaces of Earth and Mars could be carried out by small taxi vehicles that could be decelerated and accelerated by relatively small expenditures of energy.

In fact, such stable orbits do exist, and several cycling spacecraft scenarios have been proposed. Two representative concepts are the Versatile International Station for Interplanetary Transport (VISIT) cycler, which has been extensively studied by researchers at Science Applications International Corporation, and the Escalator Cycler, a proposal by "Buzz" Aldrin. These concepts, which are illustrated in Figs. 7 and 8, respectively, are discussed in more detail in Refs. 1 and 2.

The VISIT scenario uses stable orbits about the sun that have a prescribed commensurability with the Earth and Mars. For instance, the VISIT-1 orbit, illustrated in Fig. 7, goes around the sun four times while the Earth goes around five times. Hence it has a commensurability of four to five (4:5), and it re-encounters the Earth every 5 yr. With respect to Mars, VISIT-1 has a commensurability of 3:2 and re-encounters Mars every 3.75 years. The VISIT orbits repeat their encounter sequences every 15 yr and do not use gravity swingby effects for other than navigational purposes. A network of VISIT spacecraft (usually three) at different orientations in Earth-Mars space are used to provide more frequent encounters with Earth and Mars. It is characteristic of the VISIT scenario that Mars and Earth encounters occur irregularly. Hence, during the 15-yr VISIT cycle there is a large variation in outbound and inbound transit times and in Mars stay times. Even when three cycling spacecraft are used, Mars stay times can vary from 1.6 to 5.9 yr.⁸

The Escalator Cycler scenario, illustrated in Fig. 8, begins with what is essentially a high-energy free-return Mars flyby trajectory. The first Mars encounter occurs on the outbound leg. When the cycler spacecraft returns to Earth (approximately 1.5 yr after the first Mars encounter), an Earth gravity swingby maneuver is used to rotate the major axis of the orbit so that the phasing will be correct for a Mars encounter on the next outbound leg. This is the "up escalator" trajectory. A second spacecraft is then launched into a mirror image trajectory that encounters Mars on its way back from aphelion. This is the "down escalator" trajectory. Two spacecraft in such orbits provide Earth and Mars encounters every 2 yr. The

encounter velocities at Mars are, however, much higher than those associated with the VISIT trajectory, and the Escalator trajectories require significant propulsive maneuvers to stay in phase with Earth-Mars geometry.

For the initial manned missions to Mars, it is desirable to use a mission scenario that involves only well-proven technologies and does not require the establishment of an extensive infrastructure. Of the mission scenarios described earlier, four are serious contenders for initial manned missions. These are the opposition-class missions, the sprint missions (which are a subset of the opposition-class scenarios), the conventional conjunction-class missions, and the fast-transfer conjunction-class missions. Accordingly, the remainder of this investigation is devoted to comparing these four mission types from the standpoints of 1) crew exposure to reduced gravity, 2) crew exposure to space radiation, and 3) Earth departure mass. In assessing the missions from these viewpoints, the trajectory data from Ref. 2 are used for the opposition, sprint, and conventional conjunction-class missions, and data from Ref. 3 are used for the fast-transfer conjunction-class missions. Since Ref. 3 is for a different time period (2011–28) than Ref. 2 (2002–15), use is made of the fact that the Earth-Mars-sun geometry repeats approximately every 15 yr in comparing the fast-transfer conjunction missions with the other scenarios. For instance, the fast-transfer mission with a 2018 Earth departure date is assumed to have trajectory characteristics similar to those of a mission with a 2003 Earth departure date.

Exposure to Reduced Gravity

It is well established that long-term exposure to weightlessness can have serious adverse effects on human beings. What is not well understood at all is how much exposure to reduced gravity is too much. Through their MIR space station missions, the Russians have established that, with adequate exercise, astronauts can withstand 1 yr of zero gravity with relatively minor long-term effects. It is generally believed that reduced gravity (e.g., the 3/8 Earth gravity that astronauts will experience on the Martian surface) is less detrimental than zero gravity. Hence, it is possible that, during their stay at Mars, astronauts will, to a degree, recover from the deconditioning they experienced on the trip from Earth, but there is no data to prove this assertion, much less to quantify it. Many Mars mission vehicle concepts have incorporated artificial gravity (e.g., separating the vehicle into two parts placed at either end of a rotating tether) that, it is hoped, would allow long trips without deconditioning. However, the degree to which such an artificial gravity field can simulate Earth gravity is not understood. Hence, for early missions to Mars, the approach generally taken to reduced gravity exposure is "the less the better."

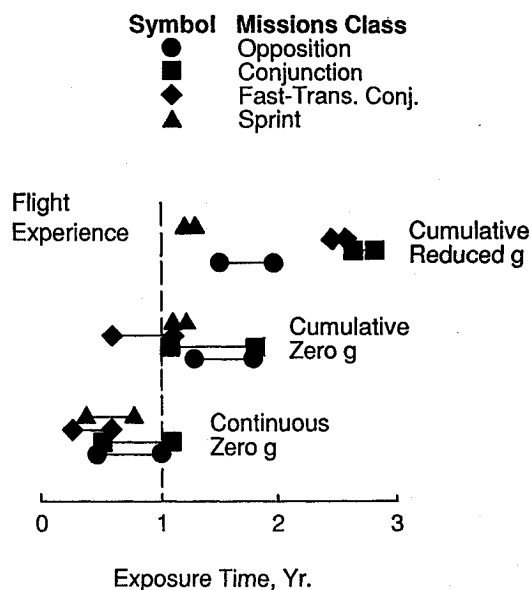


Fig. 9 Ranges of crew exposure to reduced gravity.

In Fig. 9, crew exposure to reduced gravity is displayed from three different viewpoints:

1) Continuous exposure to zero gravity: If the crew recovers completely during their stay on the Martian surface, this would be an appropriate criterion.

2) Cumulative exposure to zero gravity: If no recovery or further deconditioning occurs during the Mars stay, this would be an appropriate criterion.

3) Cumulative exposure to reduced gravity: If 3/8 gravity is as harmful as zero gravity, this criterion would be appropriate.

The results displayed in Fig. 9 are based on the mission characteristics presented in Tables 1–4. From Fig. 9, it is seen that the sprint missions satisfy all three criteria. If continuous exposure to zero gravity is the appropriate criterion, all four scenarios are acceptable. If cumulative exposure to either zero gravity or reduced gravity is the appropriate criterion, then only the sprint scenario should be considered for early Mars missions. The usefulness of the conjunction-class scenarios is seen to depend on the ability of humans to live under 3/8 gravity for long periods of time without serious deconditioning. If cumulative exposure to zero gravity is the appropriate criterion, the fast-transfer conjunction-class missions become strong candidates.

Exposure to Space Radiation

There are three primary sources of charged-particle radiation in space: 1) trapped radiation belts (such as the Van Allen belts at Earth), 2) galactic cosmic radiation, and 3) solar flares. The characteristics of these radiation sources are discussed in Refs. 9 and 10. In the present investigation, it was assumed that mission strategies would be chosen such that manned vehicles would traverse the trapped radiation belts quickly, thereby minimizing the trapped radiation dose. Previous studies have shown this to be a reasonable assumption. For instance, in Ref. 11, Nealy et al. showed that, for a typical sprint mission powered by nuclear thermal rockets, transit through the Van Allen belts accounted for approximately 1.5 rem out of a total mission dose of 39–48 rem. It should also be pointed out that nuclear propulsion systems can be effectively shielded by onboard propellants (liquid hydrogen) so that the dose from nuclear rocket firings can generally be neglected in comparison with galactic cosmic rays and solar flares.¹¹ Hence, in the present investigation only galactic cosmic radiation and solar flares are considered. There are no defined radiation dose limits for Mars missions. As an interim measure, most investigators are using the limits for low-Earth-orbit operations that were established by the National Council on Radiation Protection and Measurement (NCRP).¹² These limits are currently being revised downward and were not defined with planetary missions in mind in the first place. Hence, they are useful in comparing one mission scenario with another but are not quantitatively meaningful. In the present inves-

Table 5 Dose-equivalent limits

| Exposure time | BFO limit, rem |
|-------------------------------|----------------|
| Career ^a | |
| 30-yr-old female ^b | 140 |
| 30-yr-old male ^b | 200 |
| Annual | 50 |
| 30 day | 25 |

^aVaries with age and gender. ^bFirst exposure.

Table 6 Galactic cosmic ray BFO dose equivalent

| Location | Time of occurrence | |
|--|--------------------|-------------------|
| | Solar min, rem/yr | Solar max, rem/yr |
| Storm shelter (25-cm H ₂ O) | 28 | 13 |
| HAB module (5-cm H ₂ O) | 46 | 20 |
| Mars surface (near cliff) | 13 | 7 |

Table 7 Solar flare BFO dose equivalents, rem

| Location | Distance from the sun, AU | | |
|---|---------------------------|-----|-----|
| | 0.6 | 1.0 | 1.5 |
| Storm shelter (25-cm H ₂ O), rem | 28 | 7 | |
| Mars surface (near cliff) | | | 3 |

tigation, the NCRP blood-forming-organ (BFO) doses that are computed as the dose incurred at a 5-cm depth in tissue (simulated by H₂O) are used as a comparative basis. These limits are shown in Table 5.

In Refs. 9 and 10, the results of detailed analyses of the interaction of space radiation with matter are reported. The radiation dose assessments presented in the present paper are based on the results presented in Ref. 10.

In Ref. 10 it is pointed out that giant solar flares can produce intense bursts of radiation that could be lethal if no shielding is provided. Hence, following Ref. 11, it is assumed herein that the Mars mission vehicles are equipped with a "storm shelter" that is shielded with the equivalent of 25 cm of H₂O. The remainder of the habitation module is assumed to provide a low level of shielding equivalent to 5 cm of H₂O.

In Refs. 9 and 10 it is shown that the Martian atmosphere provides significant shielding from both solar flares and galactic cosmic rays. On the other hand, it is also shown that large amounts of Martian regolith are required to provide effective additional shielding. Accordingly, in evaluating radiation doses on the Martian surface, atmospheric shielding is taken into account, and it is assumed that the Martian habitat is located so as to be shielded by local terrain (e.g., near a cliff) but is not covered with regolith.

Giant solar flares, of a magnitude that would imperil astronauts, have occurred sporadically since they began to be quantitatively measured in the 1950s. At present, there is no reliable technique for forecasting their occurrence. Hence, manned spacecraft are usually designed to withstand the most severe recorded flares. In the present investigation, the August 1972 flare¹⁰ is used to evaluate in-transit doses, and the February 1956 flare¹⁰ is used to evaluate doses on the Martian surface since these flares are the most difficult to shield against in these respective environments. In Ref. 10, all flare doses are evaluated at a distance of 1 AU from the sun. In the present investigation, it is assumed that the solar flare dose varies inversely with the square of the distance from the sun. For flares that occur during transit, it is further assumed that the flare occurs when the spacecraft is at its closest approach to the sun. For the type II transfers (heliocentric angles greater than 180 deg) in the currently considered opposition and sprint missions this is approximately 0.6 AU.

While solar flares occur sporadically and produce doses that vary with distance from the sun, galactic cosmic radiation is evenly distributed throughout our solar system and varies (approximately sinusoidally) with time during the 11-yr solar cycle. The maximum level of galactic cosmic radiation occurs at minimum solar activity (solar minimum). The present investigation considers missions in the 2001–18 time frame. During this period, a solar minimum occurs in 2008. In the present investigation, the BFO galactic cosmic ray dose (read from plots and tables in Ref. 10) was assumed to vary sinusoidally throughout the solar cycle and linearly with time within a given year. The event doses for solar flares and annual doses from galactic cosmic radiation are summarized in Tables 6 and 7.

The data in Tables 6 and 7, along with the previously described assumptions, were applied to the opposition, conjunction, and sprint missions reported in Refs. 2 and 3 and summarized in Figs. 1–4 and Tables 1–4. To obtain an estimate of the maximum combined radiation dose in any given year, it was assumed that one giant solar flare occurred each year in addition to the galactic cosmic radiation. One 1972 flare was assumed to occur during each outbound transit at the point of closest approach to the sun. If, during the second or third years, most of the time was spent in transit,

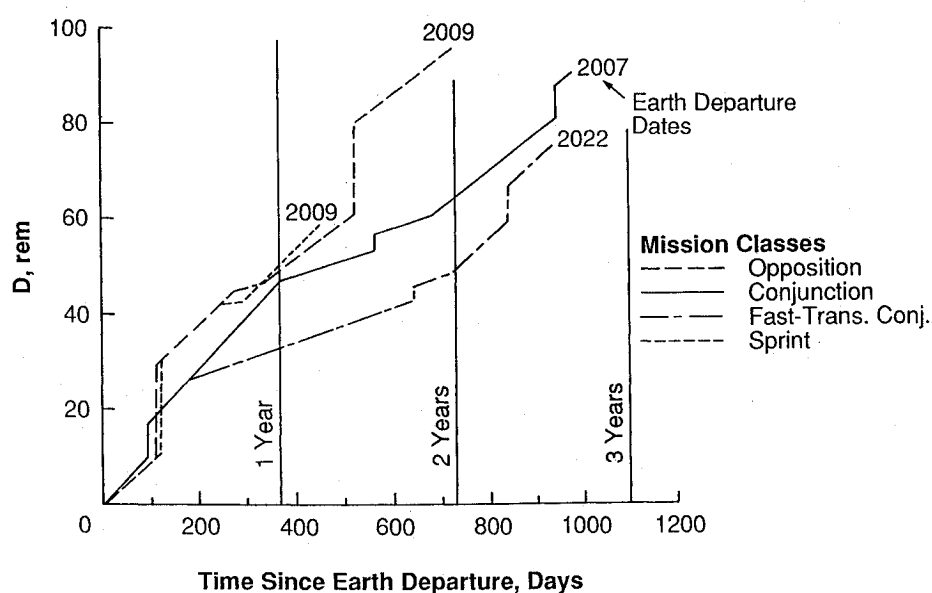


Fig. 10 Blood-forming-organ radiation doses.

Table 8 BFO radiation doses, rem

| Mission class | Earth departure date | Year | | | Mission total |
|---------------------------|----------------------|------|----|----|---------------|
| | | 1 | 2 | 3 | |
| Opposition | 2002 | 36 | 19 | — | 55 |
| | 2004 | 38 | 25 | — | 63 |
| | 2007 | 40 | 41 | — | 81 |
| | 2009 | 49 | 47 | — | 96 |
| | 2010 | 44 | 29 | — | 73 |
| | 2013 | 23 | 32 | — | 55 |
| Conjunction | 2015 | 26 | 30 | — | 56 |
| | 2003 | 20 | 10 | 22 | 52 |
| | 2005 | 35 | 19 | 33 | 87 |
| | 2007 | 47 | 17 | 26 | 92 |
| | 2009 | 33 | 13 | 22 | 68 |
| | 2011 | 24 | 11 | 22 | 57 |
| Sprint | 2014 | 25 | 10 | 24 | 59 |
| | 2016 | 28 | 13 | 26 | 67 |
| | 2018 | 33 | 17 | 35 | 85 |
| | 2002 | 36 | 04 | — | 40 |
| | 2004 | 42 | 06 | — | 48 |
| | 2006 | 49 | 08 | — | 57 |
| Fast-transfer conjunction | 2009 | 51 | 07 | — | 58 |
| | 2011 | 40 | 04 | — | 44 |
| | 2013 | 36 | 04 | — | 40 |
| | 2015 | 38 | 05 | — | 43 |
| | 2003 | 18 | 10 | 14 | 42 |
| | 2005 | 24 | 13 | 24 | 61 |
| | 2007 | 33 | 17 | 24 | 74 |
| | 2009 | 27 | 14 | 19 | 60 |
| | 2011 | 21 | 11 | 16 | 49 |
| | 2014 | 19 | 13 | 19 | 51 |
| | 2016 | 22 | 10 | 19 | 51 |

a 1972 flare was assumed to occur at closest approach to the sun. If most of the time was spent on Mars, a 1956 flare was assumed to occur while the crew was on the Martian surface at 0.0-km altitude. Because of the short duration of the sprint missions (≤ 1.26 yr), no flare was assumed to occur in the second year. The results of these calculations are summarized in Table 8 and Fig. 10 (where the worst case for each mission class is presented). Note that the worst cases (2007–09 Earth-departure dates, i.e., near solar minimum) for the opposition, sprint, and conventional conjunction-class missions all have first-year annual BFO doses that are nearly the same and closely approach the limit of 50 rem/yr. It should be noted, however, that for the worst-case fast-transfer conjunction-class mission the radiation dose in the first year is only 33 rem, well under the annual limit. The 2009 opposition-class mission also has a large (46 rem) second-year annual dose. None of the

solar flare doses, indicated by the vertical jumps in Fig. 10, exceed the 30-day limit of 25 rem, although those that occur when the vehicle is close to the sun (0.6 AU) are large, having a magnitude of approximately 19 rem. Finally, even with the extremely conservative assumption of one giant solar flare every year, none of the missions approach the career limits of 200 and 140 rem for 30-yr-old male and female astronauts, respectively. The cumulative doses for the worst-case opposition- and conjunction-class missions are large enough, however, to suggest that a given astronaut team may be limited to flying a single mission.

Initial Mass in Earth Orbit

Cost Modeling Considerations

Many investigations have used the initial mass in low-Earth orbit (IMLEO) as a primary indicator of mission feasibility and cost. Although IMLEO is certainly a meaningful indicator, it should be borne in mind that mission costs depend on many factors other than mass. To illustrate this point, typical cost-estimating relationships are discussed briefly next. The forms of the cost-estimating relationships used in this discussion are taken from the conceptual-level cost model TRANSCOST.¹³ Costs for a Mars mission may be divided into payload costs and transportation system costs, with transportation system costs being further subdivided into nonrecurring (development) costs, recurring (fabrication) costs, and operations costs. This is illustrated in Fig. 11, where the cost-estimating relationships (CERs) are also shown.

Analysis of historical cost data¹³ does show that some costs can be correlated by expressions involving vehicle stage or propulsion system dry mass raised to an appropriate power (illustrated in Fig. 11) but only when multiplying factors (such as f_1 , f_2 , f_3 , and f_4 shown in Fig. 11) are used. These multiplying factors can range from approximately 0.4 to 1.5 and hence can significantly affect cost estimates. They depend on a variety of project-peculiar characteristics, including the state of technology development, the number of development tests carried out on rocket engines, the experience of the development team with similar vehicles or systems, and the number of units to be built.

The development and fabrication CERs for the payload elements would be expected to have forms similar to those for the transportation system elements, i.e., correlated to element mass but with modifying multipliers. Some of the operations costs depend strongly on the initial mass in Earth orbit. For instance, the Earth-to-orbit (ETO) transportation costs can be computed from the number of launch vehicle flights required multiplied by the cost per launch. Propellant costs are proportional to the mass of propellants delivered to LEO, and for high-thrust systems, propellant

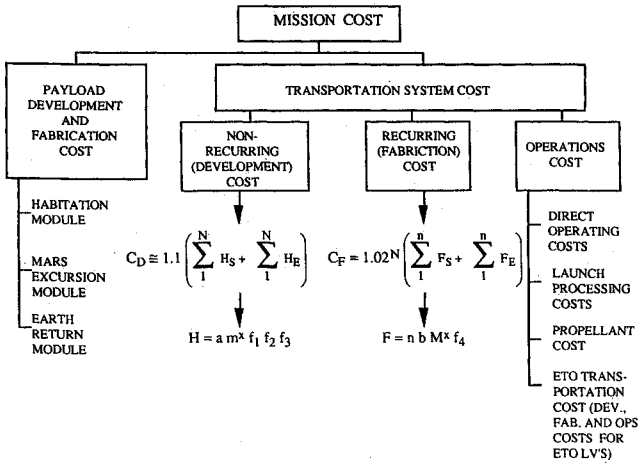


Fig. 11 Mission cost breakdown.

mass is a large fraction of the IMLEO. However, other operations costs, such as direct operating costs and launch-processing costs, may depend more strongly on factors like on-orbit assembly requirements than on IMLEO.

Hence, IMLEO is a useful rough indicator of mission cost but must be used with great care, especially when comparing very different vehicle concepts such as those employing chemical and nuclear propulsion.

Vehicle Masses at Earth Departure

At Earth departure, the vehicle stack is assumed to consist of 1) a habitation module of mass m_{HAB} , 2) a Mars excursion module (which includes the Mars lander and ascent vehicles) of mass m_{MEM} , 3) an Apollo-like Earth-return module of mass m_{ERM} , and the necessary propulsive stages and aerobrakes.

For a propulsive stage, the stage mass breakdown is approximated as

$$m = m_s + m_p + m_{p/L} \quad (1)$$

where the structure mass m_s includes engines and subsystems, and where $m_{p/L}$ is the mass of the payload to which a velocity increment must be imparted.

For an aerobraking stage, the mass breakdown is approximated by

$$m = m_{AB} + m_{p/L} \quad (2)$$

The events at which a velocity increment (or decrement) must be imparted to the vehicle during a Mars mission are identified as

- ()₁ Earth departure
- ()₂ Outbound midcourse ΔV
- ()₃ Mars arrival
- ()₄ Mars departure
- ()₅ Earth return

With the assumptions of 5% gravity losses, $m_s = 0.1m_p$, and $m_{AB} = 0.15m_{p/L}$, the rocket equation can be solved to yield the following expressions for the mass of the vehicle stack at Earth departure.

For an all-propulsive mission,

$$m_1 = \text{IMLEO} = m_{ERM} \psi_5 \psi_4 \psi_3 \psi_2 \psi_1 + m_{HAB} \psi_4 \psi_3 \psi_2 \psi_1 + m_{MEM} \psi_3 \psi_2 \psi_1 \quad (3)$$

For a mission using aerocapture at Mars and Earth,

$$m_1 = \text{IMLEO} = m_{ERM} \gamma_5 \gamma_4 \gamma_3 \gamma_2 \psi_1 + m_{HAB} \psi_4 \gamma_3 \psi_2 \psi_1 + m_{MEM} \gamma_3 \psi_2 \psi_1 \quad (4)$$

where

$$\psi = \left\{ \frac{\lambda(1-\beta)}{[(\lambda-1)\beta-\lambda]} + 1 \right\} \quad (5)$$

$$\gamma = \left(\frac{m_{AB}}{m_{p/L}} + 1 \right) = 1.15 \quad (6)$$

$$\lambda = \left(\frac{m_s}{m_p} + 1 \right) = 1.1 \quad (7)$$

$$\beta = e^{1.05 \Delta V / g I_{sp}} \quad (8)$$

In the present investigation, the following p/L masses, which are taken from Ref. 14 and are consistent with Ref. 15, are assumed.

For opposition- and conjunction-class missions:

$$m_{HAB} = 6.1 \times 10^4 \text{ kg}$$

$$m_{MEM} = 7.6 \times 10^4 \text{ kg}$$

$$m_{ERM} = 7.8 \times 10^3 \text{ kg}$$

For fast-transfer conjunction and sprint missions:

$$m_{HAB} = 4.6 \times 10^4 \text{ kg}$$

$$m_{MEM} = 7.6 \times 10^4 \text{ kg}$$

$$m_{ERM} = 7.8 \times 10^3 \text{ kg}$$

The smaller habitation module for the fast-transfer conjunction and sprint missions is justified by the significantly reduced transit times. Using the technique and the assumptions just described, Earth-departure masses were computed for the opposition, conjunction, fast-transfer conjunction, and split sprint mission scenarios using the various ΔV presented in Tables 1–4. In each case, three propulsion system options were considered: 1) all-propulsive cryogenic chemical rockets ($I_{sp} = 480$ s), 2) cryogenic chemical propulsion ($I_{sp} = 480$ s) with aerobraking at Mars and Earth, and 3) all-propulsive nuclear thermal rockets ($I_{sp} = 960$ s). The pros and cons of aerobraking and nuclear propulsion have been treated extensively in the literature and will not be repeated here. Some representative recent treatments are presented in Refs. 4 and 16–18. The results are presented in Figs. 12–15.

From Fig. 12 it is seen that, because of the high-energy transfers involved in the opposition-class missions, large Earth-departure masses are required for all-propulsive chemical vehicles. In most prior studies, an IMLEO of 1×10^6 kg has been regarded as a practical upper limit for Mars missions. The all-propulsive chemical vehicles exceed this level for all launch opportunities with the 2015 launch opportunity requiring over 3×10^6 kg. The combina-

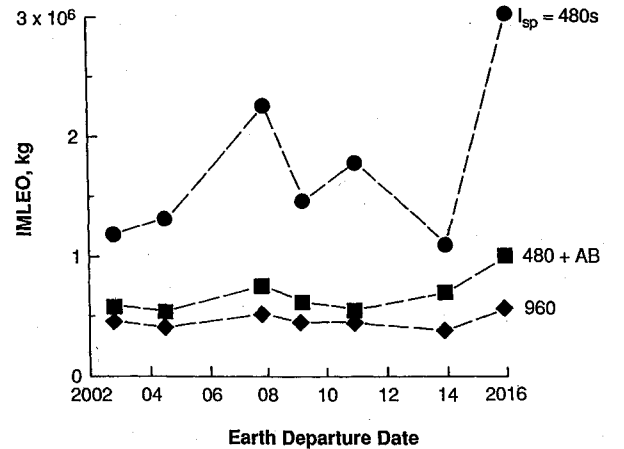


Fig. 12 Earth-departure masses for opposition-class missions.

tion of aerobraking and chemical propulsion results in significantly reduced masses. Earth-departure masses range from 0.54 to 0.77×10^6 kg except for the 2015 mission, which is an unusually energetic, short-duration mission. The use of nuclear thermal propulsion produces further significant reductions in IMLEO and results in low Earth-departure masses, ranging from 0.4 to 0.58×10^6 kg. Both chemical propulsion with aerobraking and nuclear thermal propulsion are attractive for these missions, although nuclear thermal would be the system of choice (from the standpoint of IMLEO) for the higher energy mission opportunities.

Figure 13 shows that, because of their inherently low-energy character, the conjunction-class missions have Earth-departure masses $< 1.0 \times 10^6$ kg for all three propulsion options throughout the complete cycle of mission opportunities. Again, from a mass standpoint, nuclear thermal propulsion is the system of choice. When other cost factors are considered, however, the all-propulsive chemical or chemical/aerobraking option could have lower overall mission costs. In spite of the fact that aerobraking is often thought to be of little benefit for conjunction-class missions (because of their low energies), Fig. 13 shows the combination of aerobraking and chemical propulsion to be significantly better than an all-propulsive chemical system. This is particularly true for the higher energy mission opportunities in 2014 and 2016.

In the case of the fast-transfer conjunction-class missions (Fig. 14) on the other hand, only the nuclear thermal and chemical/aerobraking options yield IMLEOs $< 10^6$ kg. The benefit of aerobraking for these missions is quite large due to the higher Mars entry velocities associated with the fast transfers. Although the nuclear thermal vehicles are always lighter, the differences in IMLEO for nuclear thermal and chemical/aerobraking are small enough to make the two quite competitive for this mission scenario.

For the split sprint missions (Fig. 15), nuclear thermal propulsion would appear to be the system of choice. Chemical propulsion with aerobraking produces IMLEOs slightly greater than 1×10^6 kg for two mission opportunities, and throughout most of the 15-yr cycle the reductions in IMLEO associated with nuclear thermal propulsion are large.

Overall, these results show that, except for the conventional conjunction class missions, all-propulsive chemical vehicles may not be feasible from a mass standpoint, and the opposition and split sprint scenarios have acceptably low IMLEOs only when nuclear

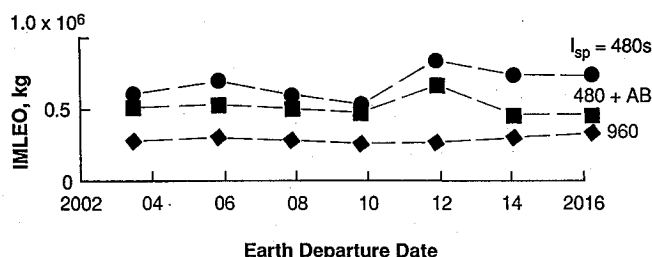


Fig. 13 Earth-departure masses for conjunction-class missions.

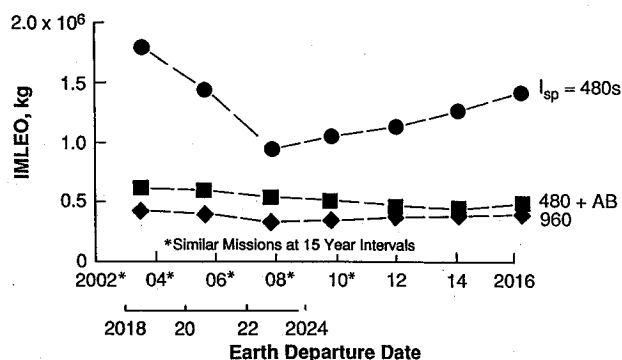


Fig. 14 Earth-departure masses for fast-transfer conjunction-class missions.

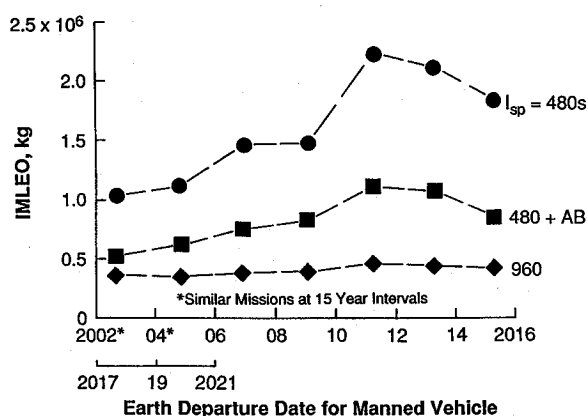


Fig. 15 Earth-departure masses for split sprint missions.

propulsion is used. On the other hand, chemical/aerobraking and nuclear vehicle systems are competitive for the fast-transfer conjunction-class missions.

Other Considerations

Although the present paper addresses three factors that could be decisive in determining the ultimate choice of mission scenario, these are by no means the only potentially important considerations. Two factors that are beyond the scope of the present paper but could be of pivotal importance are crew psychological effects during long space missions and the complex sociopolitical issue of nuclear propulsion.

Although psychological effects are much more difficult to quantify than vehicle characteristics and physiological phenomena, they certainly cannot be ignored. It is conceivable that psychological considerations¹⁹ could tilt the choice of mission scenario toward the short-duration opposition-class or split sprint missions in spite of their characteristically higher energies and Earth-departure masses. Although it is generally agreed that conjunction-class missions with long stay times on Mars will be the norm during the later "consolidation" phase of a Mars program, missions with short stay time may well be chosen for the initial manned missions. If this choice is made, there will be a strong impetus toward the development of nuclear propulsion to achieve lower Earth-departure masses shown in Figs. 12–15.

The issue of nuclear power is so sensitive politically that nuclear propulsion for Mars missions was rarely mentioned in the early 1980s despite the fact that the technology for nuclear thermal rockets is largely in hand as a result of the NERVA/ROVER program. Fortunately, nuclear propulsion is now being discussed widely as an option for Mars missions. There are still major unanswered questions, however. Even if it is a groundrule that reactors will be put in critical operation only after the vehicles have achieved nuclear-safe orbit, the issues of launch accidents and the Earth-based testing of large nuclear rockets must still be dealt with.

Concluding Remarks

Based on the analyses carried out in this investigation, the choice of mission scenario for the initial manned Mars missions depends to a large extent on the amount of physical deconditioning caused by long-term exposure to the $3/8$ Earth gravity environment of the Martian surface.

Exposure to space radiation is not a clear discriminator. If the transfer vehicle is assumed to have an adequately shielded storm shelter ($25\text{-cm H}_2\text{O}$), none of the initial mission scenarios (opposition, conjunction, fast-transfer conjunction, or split sprint) produced radiation doses significantly larger than the NCRP limits, even when conservative assumptions (one giant solar flare per year occurring at closest approach to the sun) were used. During the 2002–18 time period, the worst cases for each of the opposition, conventional conjunction, and split sprint mission opportunities produced roughly equal annual BFO radiation doses that

approached but did not significantly exceed the NCRP limits. The fast-transfer conjunction-class missions produced significantly smaller annual doses. None of the mission scenarios produced radiation doses that exceeded the 30-day or career limits. Because of their type II transfers, the opposition and sprint missions pass within approximately 0.6 AU of the sun and hence are subject to maximum solar flare doses of approximately 19 rem (compared with the NCRP 30-day limit of 25 rem). The cumulative doses for the worst-case conjunction- and opposition-class missions were approximately 100 rem, well under the NCRP career limits. Hence, from a radiation dose standpoint, the fast-transfer conjunction-class scenario is preferable, but all four scenarios are acceptable. Therefore, crew deconditioning due to exposure to reduced gravity becomes the primary discriminator.

If 3/8 Earth gravity is as harmful as zero gravity, then the appropriate criterion is cumulative exposure to reduced gravity. By this criterion, only the split sprint missions are acceptable (i.e., have cumulative exposures of approximately 1 yr or less). Although these missions are marginally feasible with chemical propulsion/aerobraking, they become truly attractive (from a mass standpoint) only with nuclear thermal propulsion.

If during their stay on the Martian surface the astronauts recover completely from in-transit zero-gravity deconditioning, then the appropriate criterion is the duration of continuous exposure to zero gravity. By this criterion, all four scenarios are acceptable since none of them exceed significantly our present flight experience of 1 yr. In this case, the conjunction-class scenarios, both conventional and fast transfer, would be preferred because of their lower Earth departure masses and the possibility of using either chemical or nuclear propulsion. If, for psychological reasons, it is desired to limit overall mission duration, the opposition-class missions would be feasible with either nuclear thermal propulsion or chemical propulsion with aerobraking.

If during their stay on Mars the astronauts experience neither recovery nor further deconditioning, the appropriate criterion is cumulative exposure to zero gravity. By this criterion, only the fast-transfer scenarios (i.e., fast-transfer conjunction and split sprint) are acceptable. Of these, the fast-transfer conjunction scenario would be preferable because of its lower IMLEOs, simplified logistics, and suitability for either chemical propulsion with aerobraking or nuclear thermal propulsion. Also, it should be recalled that, because the fast-transfer conjunction-class trajectories do not pass inside Earth orbit, the potential solar flare radiation doses are significantly lower than for the sprint trajectories. This leads to significantly lower annual radiation doses, which, although not a primary discriminator, is certainly desirable. All in all, the fast-transfer conjunction-class missions have many desirable characteristics and could be the scenario of choice for the first manned missions to Mars.

Acknowledgment

This research was funded by NASA Grant NAGW 1331 to the Mars Mission Research Center.

References

- ¹Niehoff, J. C., "Pathways to Mars: New Trajectory Opportunities," American Astronomical Society, AAS Paper 86-172, June 1988.
- ²Hoffman, S. J., McAdams, J. V., and Niehoff, J. C., "Round Trip Trajectory Options for Human Exploration of Mars," American Astronomical Society, AAS Paper 89-201, July 1989.
- ³Solder, J. K., "Round Trip Mars Trajectories: New Variations on Classic Mission Profiles," AIAA Paper 90-3794, Aug. 1990.
- ⁴Braun, R. D., Powell, R. W., and Hartung, L. C., "Effect of Interplanetary Options on a Manned Mars Aerobrake Configuration," NASA TP 3019, Aug. 1990.
- ⁵Melbourne, W. G., "Interplanetary Trajectories and Payload Capabilities of Advanced Vehicles," Jet Propulsion Lab., TR 32-68, Pasadena, CA, March 1961.
- ⁶Hack, K. J., George, J. A., and Dudzinski, L. A., "Nuclear Electric Propulsion Mission Performance for Fast Piloted Mars Missions," AIAA Paper 91-3488, Sept. 1991.
- ⁷Zubrin, R., and Baker, D., "Humans to Mars in 1999," *Aerospace America*, Vol. 28, No. 8, 1990, pp. 31-41.
- ⁸Hoffman, S. J., Friedlander, A. L., and Nock, K. T., "Transportation Mode Performance, Comparison for a Sustained Manned Mars Base," AIAA Paper 86-2016, Aug. 1986.
- ⁹Simonsen, L. C., Nealy, J. E., Townsend, L. W., and Wilson, J. W., "Radiation Exposure for Manned Mars Surface Missions," NASA TP 2979, March 1990.
- ¹⁰Simonsen, L. C., and Nealy, J. E., "Radiation Protection for Human Missions to the Moon and Mars," NASA TP 3079, Feb. 1991.
- ¹¹Nealy, J. E., Simonsen, L. C., Wilson, J. W., Townsend, L. W., Qualls, G. D., Schnitzler, B. G., and Gates, M. M., "Radiation Exposure and Dose Estimates for a Nuclear-Powered Manned Mars Sprint Mission," Eighth Symposium on Space Nuclear Power Systems, Albuquerque, NM, Jan. 6-10, 1991.
- ¹²Anon., "NCRP-98: Guidance on Radiation Received in Space Activities," National Council on Radiation Protection and Measurement, Bethesda, MD, July 1989.
- ¹³Koelle, D. E., "TRANSCOST: Statistic-Analytical Model for Cost Estimation and Economic Optimization of Space Transportation Systems," MBB Rept. URV-180 (88), MBB Space and Communications and Propulsion Systems Div., Munich, Germany, Oct. 1988.
- ¹⁴Freeman, D. C., Powell, R. W., and Braun, R. D., "Manned Mars Aerobrake Vehicle Design Issues," International Astronautical Federation, IAF Paper 90-197, Oct. 1990.
- ¹⁵"Report of the 90-Day Study on Human Exploration of the Moon and Mars," NASA, Nov. 1989.
- ¹⁶Walberg, G. D., "Aerocapture for Manned Mars Missions—Status and Challenges," AIAA Paper 91-2870, Aug. 1991.
- ¹⁷Bennett, G. L., Graham, S. R., and Harer, K. F., "Back to the Future—Using Nuclear Propulsion to Go to Mars," AIAA Paper 91-1888, June 1991.
- ¹⁸Clark, J. S., and Miller, T. J., "The NASA/DOE/DOD Nuclear Rocket Propulsion Project: FY1991 Status," AIAA Paper 91-3413, Sept. 1991.
- ¹⁹Calvin, M., and Gagenko, O. (eds.), "Foundations of Space Biology and Medicine," Joint NASA/USSR Academy of Sciences publication, NASA-SP-374, Vol. 1, 1975.

Ronald K. Clark
Associate Editor